6524 *Chem. Mater.* **2010,** *22,* 6524–6528
DOI:10.1021/cm101389v

CHEMISTRY OF MATERIALS
Article

Tunable Size and Shape Control of Platinum Nanocrystals from a Single Peptide Sequence

Lauren M. Forbes,[†,‡] Andrew P. Goodwin,[†] and Jennifer N. Cha*[,†]

[†]*Department of Nanoengineering and* [‡]*Department of Chemistry and Biochemistry, 9500 Gilman Drive, University of California, San Diego, La Jolla, California 92093-0448, United States*

Received May 17, 2010. Revised Manuscript Received August 10, 2010

Nanoscale platinum architectures have been extensively studied as potential materials for applications in catalysis and fuel cells. Due to the high cost of platinum, much of the research has been geared toward developing methods to obtain monodisperse, monomorphic nanocrystals smaller than 10 nm. Peptide-mediated synthesis of inorganic materials is an attractive alternative to colloidal synthesis because it can be performed under ambient conditions and the peptides can be removed from the metal surfaces at mild pH or in the presence of enzymes. As a first step to achieve size and shape-controlled nanocrystals using peptides, we demonstrate here (a) the isolation of peptides that bind to specific crystal planes of platinum and (b) that a single peptide can produce structures ranging from sub-2 nm seed crystals to monodisperse 4 nm platinum polyhedra to 7 to 8 nm platinum cubes simply by changing the rates of metal reduction. This work demonstrates the first steps toward achieving biochemical control of platinum nanocrystal synthesis.

In recent years, the design and synthesis of nanoscale platinum architectures have been explored extensively for applications ranging from heterogeneous catalysis to fuel cells.[1−5] To obtain homogeneous catalytic activities while minimizing precious metal costs, research has focused on the development of efficient, facile methods to synthesize monodisperse sub-10 nm nanocrystals while exercising accurate shape control.[6−15] Platinum nanocrystals can be synthesized with relatively controlled sizes and morphologies through mediation by a surfactant or polymer. However, the use of ligands that show affinity for specific crystal plane may allow synthesis of more catalytically potent morphologies. Inorganic-binding biomolecules, such as peptides, have excellent potential as a class of morphology-specific ligands due to their variety of available amino acid sequences,[16−25] but it has proven very difficult to controllably produce monodisperse and monomorphic nanocrystals from peptides with tunable size and shape. We report here the controlled synthesis of platinum nanocrystals with a variety of sizes and morphologies from a single peptide sequence at room temperature. After isolating a peptide designed to bind a specific crystal plane of platinum by phage display, we produced structures ranging from sub-2 nm seed crystals to monodisperse 4 nm platinum polyhedra to 7 to 8 nm platinum cubes using simply the change in the rates of metal reduction. Syntheses with mismatched or no peptide led to ill-defined nanoparticles and bulk aggregates. This work illustrates the first steps toward achieving controlled

*To whom correspondence should be addressed. E-mail: jencha@ucsd.edu.

(1) Prabhuram, J.; Wang, X.; Hui, C. L.; Hsing, I.-M. *J. Phys. Chem.* **2003**, *107*, 11057–11064.
(2) Mukerjee, S. *J. Appl. Electrochem.* **1990**, *20*, 537–548.
(3) Song, H.; Rioux, R. M.; Hoefelmeyer, J. D.; Komor, R.; Niesz, K.; Grass, M.; Yang, P. D.; Somorjai., G. A. *J. Am. Chem. Soc.* **2006**, *128*, 3027–3029.
(4) Gennett, R.; Landi, B. J.; Elich, J. M.; Jones, K. M.; Alleman, J. L.; Lamarre, P.; Morris, R. S.; Raffaelle, R. P.; Heben, M. J. *Mater. Res. Soc. Symp. Proc.* **2003**, *756*, FF5.8.1–FF5.8.6.
(5) Brandon, N. P.; Skinner, S.; Steele, B. C. H. *Annu. Rev. Mater. Res.* **2003**, *33*, 183–213.
(6) Lee, H.; Habas, S. E.; Kweskin, S.; Butcher, D.; Somorjai, G. A.; Yang, P. *Angew. Chem., Int. Ed.* **2006**, *118*, 7988–7992.
(7) Ahmadi, T. S.; Wang, Z. L.; Henglein, A.; El-Sayed, M. A. *Chem. Mater.* **1996**, *8*, 1161–1163.
(8) Song, H.; Kim, F.; Connor, S.; Somorjai, G. A.; Yang, P. *J. Phys. Chem. B* **2005**, *109*, 188–193.
(9) Wang, C.; Daimon, H.; Onodera, T.; Koda, T.; Sun, S. A. *Angew. Chem., Int. Ed.* **2008**, *47*, 3588–3591.
(10) Tian, N.; Zhou, Z.-Y.; Sun, S.-G.; Ding, Y.; Wang, Z. L. *Science* **2007**, *316*, 732–735.
(11) Park, S.; Xie, Y.; Weaver, M. J. *Langmuir* **2002**, *18*, 5792–5798.
(12) Sharma, R. K.; Sharma, P.; Maitra, A. *J. Colloid Interface Sci.* **2003**, *265*, 134–140.
(13) Somorjai, G. A.; Blakely, D. W. *Nature* **1975**, *258*, 580–583.
(14) Narayanan, R.; El-Sayed, M. A. *Nano Lett.* **2004**, *4*, 1343–1348.
(15) Sun, S.-G.; Chen, A.-C.; Huang, T.-S.; Li, J.-B.; Tian, Z.-W. *J. Electroanal. Chem.* **1992**, *340*, 213–226.
(16) Thompson, J. B.; Paloczi, G. T.; Kindt, J. H.; Michenfelder, M.; Smith, B. L.; Stucky, G.; Morse, D. E.; Hansma, P. K. *Biophys. J.* **2000**, *79*, 3307–3312.
(17) Addadi, L.; Weiner, S. *Proc. Natl. Acad. Sci.* **1985**, *82*, 4110–4114.
(18) Cha, J. N.; Stucky, G. D.; Morse, D. E.; Deming, T. J. *Nature* **2000**, *403*, 289–292.
(19) Naik, R. R.; Stringer, S. J.; Agarwal, G.; Jones, S. E.; Stone, M. O. *Nat. Mater.* **2002**, *1*, 169–172.
(20) Gugliotti, L. A.; Feldheim, D. L.; Eaton, B. E. *Science* **2004**, *304*, 850–852.
(21) Gugliotti, L. A.; Feldheim, D. L.; Eaton, B. E. *J. Am. Chem. Soc.* **2005**, *127*, 17814–17818.
(22) Li, Y.; Whyburg, G. P.; Huang, Y. *J. Am. Chem. Soc.* **2009**, *131*, 15998–15999.
(23) Li, Y.; Huang, Y. *Adv. Mater.* **2010**, *22*, 1921–1925.
(24) Pacardo, D. B.; Sethi, M.; Jones, S. E.; Naik, R. R.; Knechtt, M. R. *ACS Nano* **2009**, *3*, 1288.
(25) Bassindale, A. R.; Codina-Barrios, A.; Frascione, N.; Taylor, P. G. *Chem. Commun.* **2007**, 2956–2958.

Published on Web 11/24/2010

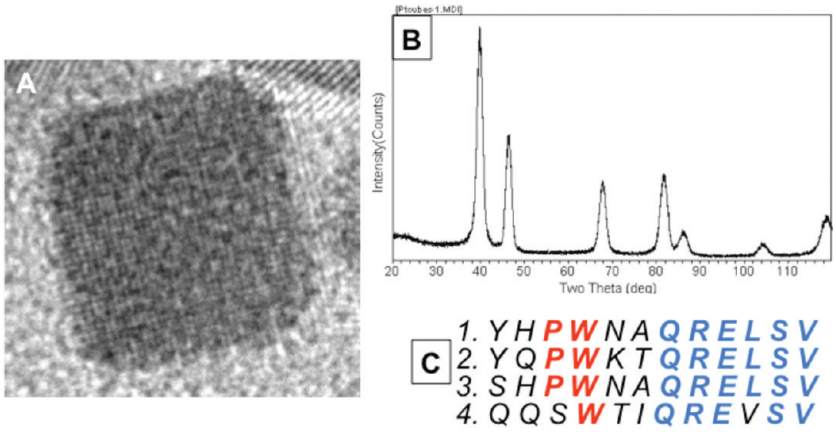

Figure 1. (A) TEM image of synthetic platinum nanocubes via literature prep.[9] Phages were screened against cleaned thin films of these cubic nanocrystals. (B) Powder XRD pattern of synthesized nanocrystals. (C) Amino acid consensus sequences of peptides obtained after three rounds of screening against the platinum nanocubes.

syntheses of platinum nanocrystals of tunable sizes and morphologies from a single peptide sequence.

Peptides that bind a single crystal plane of platinum were isolated using a variant of phage display, a facile and oft-applied method to find peptides that bind specific substrates.[19−28] The reason to screen against a single crystal plane of platinum was to obtain homologous sequences that would bind specifically to Pt (100), thereby providing a peptide sequence that would template specifically to this crystal plane. Because combinatorial screening against bulk dispersed heterogeneous powders of various metals, sputter, or electrodeposited polycrystalline planar substrates would expose the bacteriophage library to multiple metal crystal planes and lead to isolation of peptides with nonspecific binding, phage libraries were screened against Pt (100) alone instead.[27] Due to the extremely high cost of obtaining single crystal platinum, monodisperse cubic platinum nanocrystals bound by Pt (100) were first prepared using published surfactant-templated colloidal syntheses.[9] X-ray diffraction (XRD) showed the high crystalline quality, and high-resolution electron microscopy (HRTEM) showed that the cubic nanocrystals were indeed bound by (100) planes (Figure 1A,B). Following previously reported procedures, the platinum nanocubes were next dried onto silicon substrates by slow evaporation to create well-ordered packed arrays of platinum nanocrystals and treated with UV/O_2 for 1 h to remove the top layer of capping ligands.[9] Solutions of the phage library (NEB, Ph.D. 12) composed of 10^9 different peptide sequences were then carefully dropped onto the cleaned platinum nanocrystal substrates. After incubation for 2 h in a humid environment, unbound phage was removed with a pipet and the platinum surfaces were gently rinsed with Tween 20 solutions. Phage bound to the substrate were eluted at pH 2 and amplified for a second screening against new UV/O_2-cleaned and oriented platinum nanocrystal films. After three consecutive rounds, the amino acid sequences of the peptides that bound to the Pt (100) platinum nanocrystal substrates were determined through DNA extraction of select phage. As shown in Figure 1C, because the starting platinum substrates were highly crystalline and contained mostly a single crystal plane, significant amino acid homology between the sequences was observed, with a consensus sequence of Pro-Trp-X-X-Gln-Arg-Glu-Leu-Ser-Val (PWxxQRELSV); additional obtained sequences are shown in Supplementary Figure 1 (Supporting Information). While the exact role each amino acid plays on binding platinum is currently being investigated, the generation of a clear consensus sequence indicates binding to a single crystal substrate. The overall isoelectric points of the peptides were close to neutral with values ranging from ~6.7 to 8.5.

Next, we explored the ability of the isolated peptides to mediate nanocrystal synthesis. First, the peptide sequence Tyr-Gln-Pro-Trp-Lys-Thr-Gln-Arg-Glu-Leu-Ser-Val (YQPWKTQRELSV) was chosen at random and obtained commercially. The synthesized peptides were terminated with free carboxy and amine ends and provided as a trifluoroacetic acid (TFA) salt. The calculated pI of the peptide chosen for the studies would, therefore, be ~8.5 and roughly have a net charge of +1 at pH 7.0. Varying concentrations of peptide and Pt^{2+} precursors (K_2PtCl_4 or $Pt(NH_3)_4(NO_3)_2$) were incubated in either deioinzed water or 20 mM Tris buffer for 5−15 min at room temperature with constant stirring, followed by rapid addition of five molar equivalents of sodium borohydride ($NaBH_4$) to Pt^{2+}. Aliquots were removed at time intervals ranging from 10 to 30 min and analyzed by electron microscopy. As shown in Figure 2A, in the presence of K_2PtCl_4, fast reduction by $NaBH_4$ produced extremely small (1 to 2 nm) platinum nuclei from the soluble platinum-binding peptides with no particles of any defined morphology (Figure 2A). These nuclei were obtained almost irrespective of the molar ratio of K_2PtCl_4 to peptide (25:1 through 250:1). When smaller molar ratios of K_2PtCl_4/peptide were used, the addition of peptide to the platinum solution immediately yielded white

(26) Sarikaya, M.; Tamerler, C.; Jen, A. K.-Y.; Schulten, K.; Baneyx, F. *Nat. Mater.* **2003**, *2*, 577–585.
(27) Whaley, S. R.; English, D. S.; Hu, E. L.; Barbara, P. F.; Belcher, A. M. *Nature* **2000**, *405*, 665–668.
(28) Mao, C.; Solis, D. J.; Reiss, B. D.; Kottmann, S. T.; Sweeney, R. Y.; Hayhurst, A.; Georgiou, G.; Iverson, B.; Belcher, A. M. *Science* **2004**, *303*, 213–217.

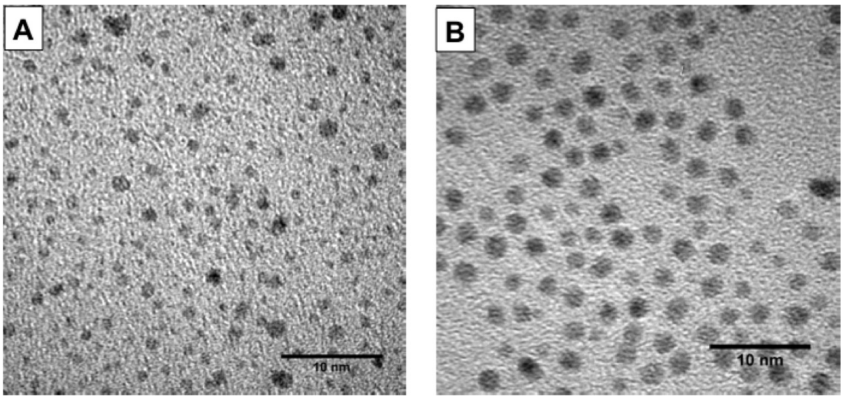

Figure 2. (A) 1 to 2 nm platinum nanocrystals synthesized from platinum binding peptides and K_2PtCl_4 and $NaBH_4$. (B) 4 nm polyhedra platinum nanocrystals synthesized from platinum binding peptides and $Pt(NH_3)_4(NO_3)_2$ and $NaBH_4$. Scale bars in both images are 10 nm.

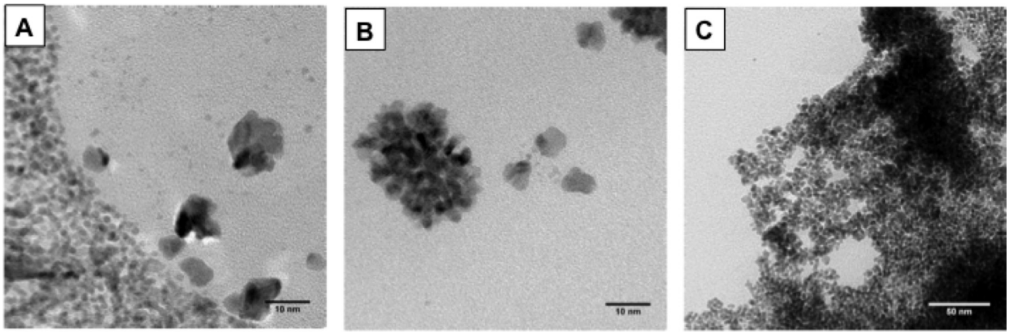

Figure 3. (A) Bulk platinum precipitates using $Pt(NH_3)_4(NO_3)_2$ and silver binding peptides. (B) Bulk platinum precipitates using $Pt(NH_3)_4(NO_3)_2$ and no peptides. (C) Bulk platinum precipitates using K_2PtCl_4 and no peptides. All reactions were run using $NaBH_4$ as the reductants.

precipitates that became a slight tan upon reduction with nothing observable by transmission electron microscopy (TEM). In contrast to the K_2PtCl_4 reactions, when the Pt (100) platinum binding peptides were mixed with the less reactive $Pt(NH_3)_4(NO_3)_2$ at 25:1 Pt^{2+}/peptide ratios at pH 7 and reduced by $NaBH_4$, well-defined 3 to 4 nm platinum polyhedra nanocrystals were produced (Figure 2B). The sizes and shape distributions remained consistent up to 250:1 $Pt(NH_3)_4(NO_3)_2$ to peptide ratios, and the use of either 20 mM Tris buffer (pH 7) or water did not affect particle synthesis. At higher molar ratios of $Pt(NH_3)_4(NO_3)_2$, particle formation was uncontrolled in both size and morphology and many particles aggregated. Using a different inorganic binding peptide, the silver binding NH_2-Asn-Pro-Ser-Ser-Leu-Phe-Arg-Tyr-Leu-Pro-Ser-Asp-COOH (NPSSLFRYLPSD)[19] yielded bulk aggregates with no individual well-defined nanocrystals (Figure 3A,B) for both Pt^{2+} sources; these were similar to that observed when no peptides were used at all (Figure 3C).

The clear discrepancy in nanoparticle sizes obtained when using $Pt(NH_3)_4(NO_3)_2$ instead of K_2PtCl_4 with the platinum binding peptides implied that the rate of metal reduction might play a key role in controlling the size and morphology of the resultant particles. Rapid nucleation with K_2PtCl_4 and $NaBH_4$ led to the formation of only small seed nuclei with no subsequent growth. With a less reactive platinum species such as the ligand stabilized $Pt(NH_3)_4(NO_3)_2$, the slower nucleation led to larger 4 nm particles with narrow size distributions and spherical (polyhedral) shape. Thus, we hypothesized that slowing the rate of metal reduction further would lead to larger particles and different morphologies. To test this, hydrogen gas was used as a slower reductant to decrease the rate of metal reduction even further. Peptide/K_2PtCl_4 solutions were first purged with nitrogen for 5 min and then hydrogen for another 5 min and then immediately sealed and left to sit overnight with no stirring. Instead of the 1 to 2 nm nuclei obtained previously using K_2PtCl_4, 7 to 8 nm platinum nanocrystals showing cube and truncated cube morphologies were obtained (Figure 4). Statistical analyses of 617 particles from the hydrogen synthesis showed the nanocrystals to be relatively heterogeneous in size and shape, ranging in dimensions from 6 to 8 nm and roughly 20% cubic, 35% truncated cubic, and the rest a mixture of octahedral, tetrahedral, and spherical. For these syntheses, the optimal molar ratio of platinum to peptide appeared to be 1:1; smaller amounts of K_2PtCl_4 yielded no observable reduced platinum by TEM while larger K_2PtCl_4/peptide ratios (25:1) caused the formation of larger structures composed of aggregated small particles (Supplementary Figure 2, Supporting Information). When the more stable $Pt(NH_3)_4(NO_3)_2$ was used instead of K_2PtCl_4 in the hydrogen reactions, no Pt(0) structures of any kind were observed within 16 h. As with previous trials, syntheses without peptide or with silver binding peptide, hydrogen reduction of K_2PtCl_4 yielded only bulk aggregates (Supplementary Figure 3, Supporting Information). Since one of the purposes of screening phage libraries against

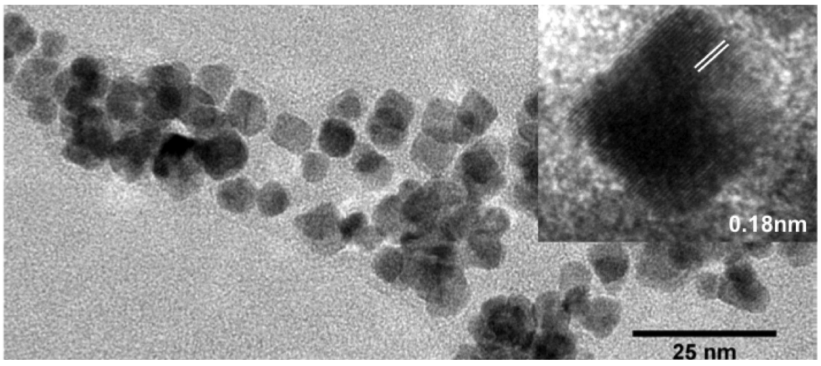

Figure 4. TEM image of 7 to 8 nm truncated cubic and cubic platinum nanocrystals obtained by reacting the platinum (100) binding peptides with K_2PtCl_4 in hydrogen for 16 h. Inset figure shows the Pt (100) lattice fringes.

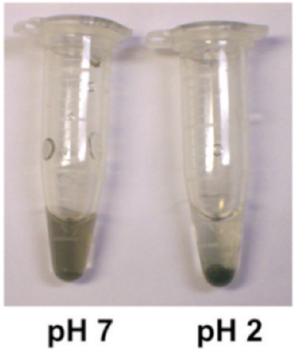

Figure 5. Peptide stabilized platinum nanoparticles at pH 7 (left) and after changing the pH to 2 (right).

bare Pt (100) surfaces was to bias the preferential stabilization of the peptides at the (100) face, the successful generation of cubic morphologies enables us to investigate the feasibility of controlling crystal morphology through peptides that interact with specific crystal planes.[29] This ability to use biomolecular recognition to tune crystal shape would be an exciting advance in nanocrystal synthesis.

While the peptide stabilized platinum nanocrystals seemed remarkably stable and well-dispersed for many days and weeks, decreasing the pH of the solutions to 2 caused all of the particles to immediately preciptate and aggregate from solution (Figure 5). This most likely is due to disassociation of the peptide from the platinum surfaces at acidic pH, which is consistent with the phage elution process at pH 2. This observation further substantiates the peptides' involvement in the nanocrystal synthesis as capping ligands. Furthermore, these results show that it is possible to use simple changes in pH to strip surface bound peptides from the platinum nanocatalysts, exposing their active faces. Since proton exchange membrane fuel cells usually require stability at low pH, studies are also currently underway to isolate peptides that can be dissociated from platinum at basic pH.

To obtain optimal catalytic activities in platinum nanocrystals, it is imperative to be able to accurately control the particle size and shape.[30] However, current ligand design limits the potential complexity of what can be synthesized in bulk. This report demonstrates that platinum nanocrystals with specific morphologies and sizes can be controllably synthesized from a rationally isolated single peptide sequence by tuning the rate of metal reduction and nanocrystal nucleation. When the highly reactive precursor K_2PtCl_4 is rapidly reduced by hydrides, leading to high supersaturation and a large number of initial nuclei, very small seed particles are formed that are quickly stabilized by the peptides. Decreasing the rates of metal reduction through more stable Pt precursors, such as $Pt(NH_3)_4(NO_3)_2$, or less reactive reductants, such as H_2, leads to a smaller number of nucleation seeds and larger particles, generating monodisperse 4 nm platinum polyhedra and 7 to 8 nm cubes, respectively. These results clearly show that the judicious choice of synthesis parameters can lead to the isolation of platinum nanostructures with defined morphologies and sizes from peptides at room temperature and no other metal additives. We plan to expand the power of peptide-mediated synthesis by isolating peptides that bind to other crystal planes of platinum and determine their influence on nanocrystal growth, possibly enabling us to synthesize platinum nanocrystals of complex morphologies that have not yet been made.

Experimental Section

Preparation of Pt Cubes for Phage Screening. Cubic platinum nanocrystals were prepared using published methods.[9] All of the nanoparticles were analyzed by scanning transmission electron microscopy (STEM), scanning electron microscopy (SEM), TEM, and XRD. To prepare substrates for phage display, 50 μL of a solution of the nanoparticles in 1:1 octane/hexane was slowly evaporated on a clean piece of silicon. The particles were then cleaned by UV/O_2 for 1 h to remove surfactants.

Phage Display. Fifty microliters (10 μL of phage library in 40 μL of 0.1% Tris Buffered Saline Tween (TBST)) was placed on a prepared platinum nanocrystal substrate and allowed to incubate for 2 h, after which the drop was removed and discarded. The substrate was washed 6 times with 50 μL of 0.1% TBST. The bound phages were then eluted using 2 consecutive 30 minute rinses with 0.2 M glycine and 1 mg/mL BSA (pH 2) solutions. The glycine solutions were then combined and neutralized with 1 M Tris (pH 9). Eluted phage were amplified,

(29) Ren, J.; Tilley, R. D. *J. Am. Chem. Soc.* **2007**, *129*, 3287–3291.
(30) Chen, J.; Lima, B.; Lee, E. P.; Xia., Y *Nanotoday* **2009**, *4*, 81–95.

and two more rounds of panning were performed. Bacteriophage DNA was extracted from round 2 and 3 phages for sequencing.

Peptide Mediated Platinum Nanoparticle Synthesis. For platinum nanocrystal synthesis, peptide solutions (3×10^{-5} M) were added to $Pt(NH_3)_4(NO_3)_2$ or K_2PtCl_4 (7.5×10^{-4} to 7.5×10^{-3} M) in water or 20 mM Tris buffer (pH 7) in a 1.5 mL Eppendorf tube. The solutions were stirred for 5 min, and then, 5 mol equiv of $NaBH_4$ relative to platinum were added. The solution is then rapidly stirred for 1 h. Reactions (1−4 μL) were dried on TEM grids for microscopy.

Peptide Mediated Platinum Nanoparticle Synthesis−Hydrogen Reduction. Peptide solutions (1.5×10^{-5}, 8×10^{-6}, and 4×10^{-7} M) were added to 10 mL solutions of 1×10^{-5} M aged K_2PtCl_4(aq) in water. Nitrogen was bubbled through the solution for 20 min, followed by bubbling hydrogen for 5 min. The flask was sealed and allowed to react for 12 h at room temperature. Reactions (1−4 μL) were dried on TEM grids for microscopy.

Acknowledgment. We acknowledge support from the NSF award (CMMI-0856671) and UCSD start up funds. We thank Prof. Kenneth Vecchio and Dr. Norm Olson for TEM support and assistance. We acknowledge the use of the UCSD Cryo-Electron Microscopy Facility which is supported by NIH grants to Dr. Timothy S. Baker and a gift from the Agouron Institute to UCSD.

Supporting Information Available: Figures of sequences isolated from Pt (100) binding phage, platinum structures, and magnification images of platinum structures (PDF). This material is available free of charge via the Internet at http://pubs.acs.org.